Determination of electroweak parameters in polarised DIS at HERA

arXiv:1806.01176
Submitted to EPJC

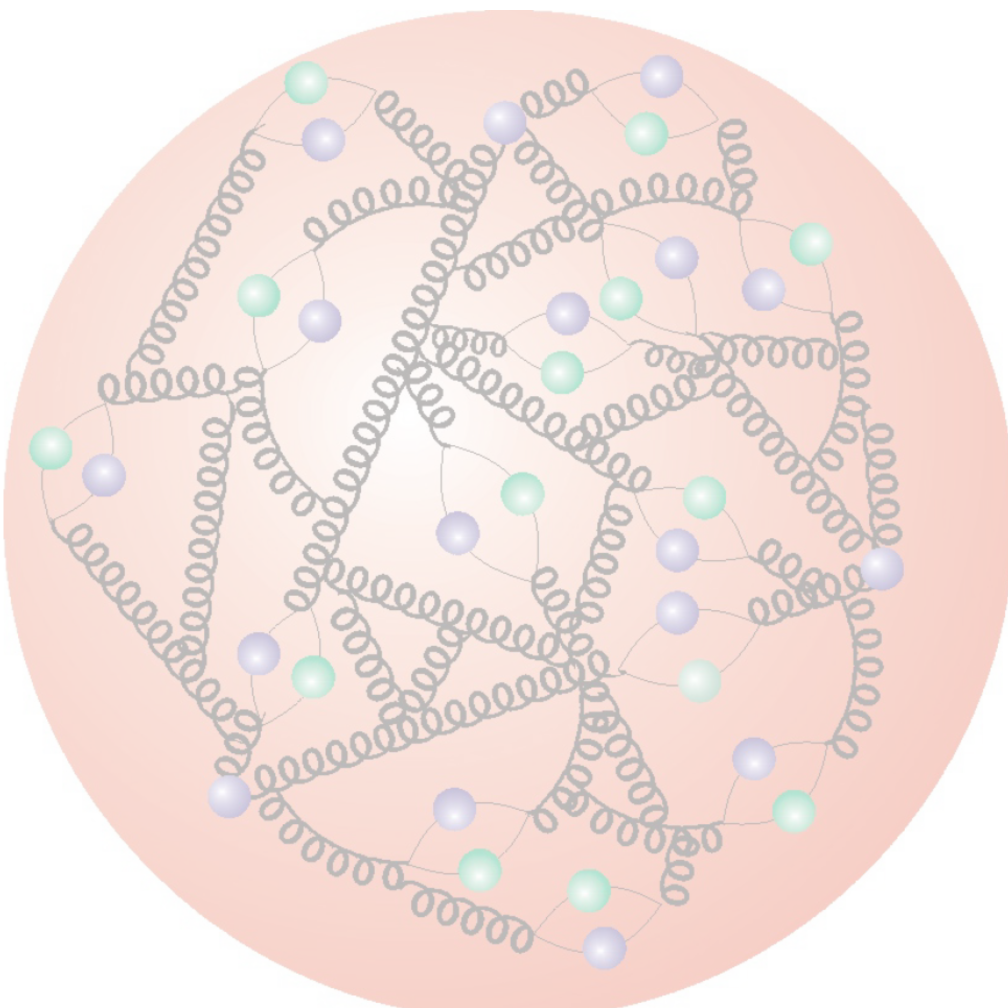

- Deep Inelastic Scattering
- EW Couplings & PDFs
- H1 Detector & Selection
- Fit Methodology
- Neutral & Charged Current Weak Coupling Fits
- BSM Form Factor Deviations in NC and CC DIS

Eram Rizvi
Queen Mary
University of London

QCD@LHC
— Dresden —
27th August 2018

Deep Inelastic Scattering

Neutral current scattering

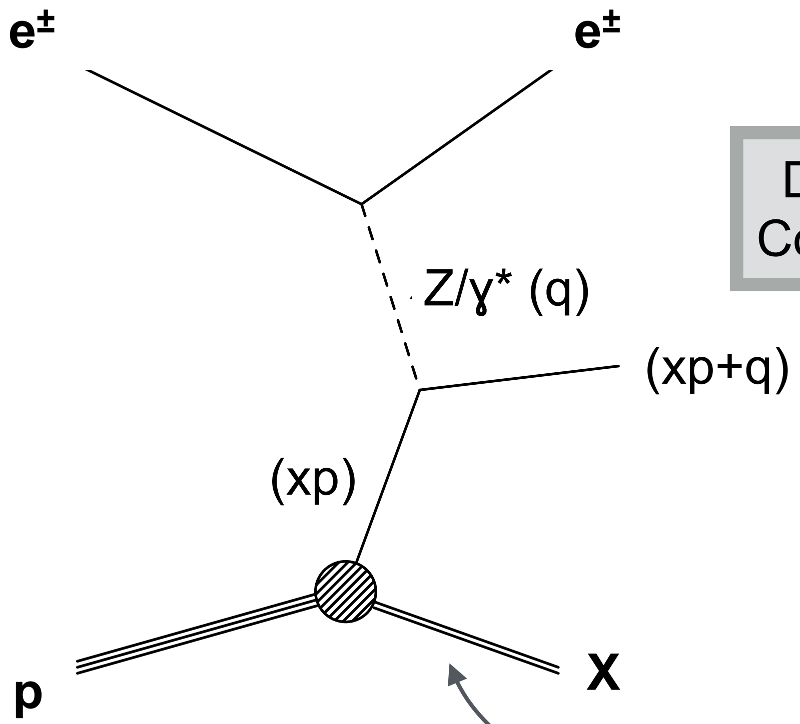

Charged current scattering

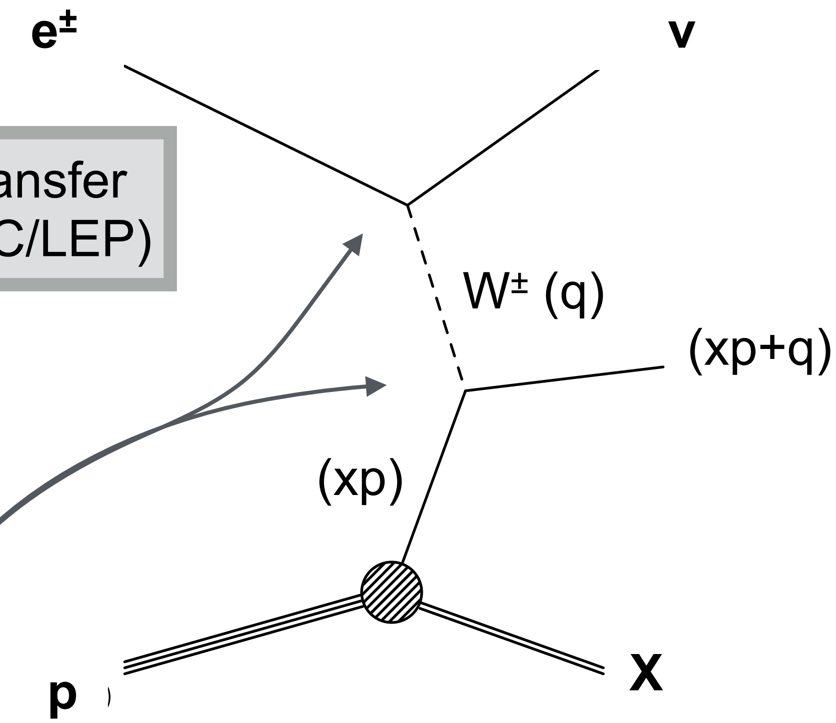

DIS tests space-like 4-momentum transfer
Complementary to time-like tests (LHC/LEP)

Factorisation in ep collisions: $\sigma_{ep\to eX} = f_{p\to i} \otimes \hat{\sigma}_{ei\to eX}$

$xf_{p\to i}$ = quark / gluon momentum density in proton: parton density function (PDFs)

Use factorisation in pp collisions at LHC: $\sigma_{pp\to X} = f_{p\to i} \otimes \hat{\sigma}_{i,j\to X} \otimes f_{p\to j}$

Signature
Isolated electron/positron
pT balanced with hadronic system X

Signature
No detected lepton (neutrino)
pT imbalanced for hadronic system X

PDFs are not observables - only structure functions are

Measuring these cross sections allows indirect access to the universal PDFs $xf_{p\to i}$

Structure Functions

neutral current	$\frac{d\sigma^{\pm}_{NC}}{dxdQ^2} = \frac{2\pi\alpha^2}{x} \left[\frac{1}{Q^2}\right]^2 \left[Y_+\tilde{F}_2 \mp Y_- x\tilde{F}_3 - y^2\tilde{F}_L\right]$
charged current	$\frac{d\sigma^{\pm}_{CC}}{dxdQ^2} = \frac{G_F^2}{4\pi x} \left[\frac{M_W^2}{M_W^2+Q^2}\right]^2 \left[Y_+\tilde{W}_2^{\pm} \mp Y_- x\tilde{W}_3^{\pm} - y^2\tilde{W}_L^{\pm}\right]$

$$Y_{\pm} = 1 \pm (1-y)^2$$

$\tilde{F}_2 \propto \sum (xq_i + x\bar{q}_i)$	Dominant contribution
$x\tilde{F}_3 \propto \sum (xq_i - x\bar{q}_i)$	Only sensitive at high $Q^2 \sim M_Z^2$
$\tilde{F}_L \propto \alpha_s \cdot xg(x,Q^2)$	Only sensitive at low Q^2 and high y

similarly for pure weak CC analogues:

$W_2^{\pm}$, $xW_3^{\pm}$ and $W_L^{\pm}$

The NC reduced cross section defined as:

$$\tilde{\sigma}^{\pm}_{NC} = \frac{Q^2 x}{2\alpha\pi^2}\frac{1}{Y_+}\frac{d^2\sigma^{\pm}}{dxdQ^2}$$

$$\tilde{\sigma}^{\pm}_{NC} \sim \tilde{F}_2 \mp \frac{Y_-}{Y_+} x\tilde{F}_3$$

The CC reduced cross section defined as:

$$\sigma^{\pm}_{CC} = \frac{2\pi x}{G_F^2}\left[\frac{M_W^2+Q^2}{M_W^2}\right]^2 \frac{d\sigma^{\pm}_{CC}}{dxdQ^2}$$

$$\frac{d\sigma^{\pm}_{CC}}{dxdQ^2} = \frac{1}{2}\left[Y_+ W_2^{\pm} \mp Y_- xW_3^{\pm} - y^2 W_L^{\pm}\right]$$

Kinematic Range

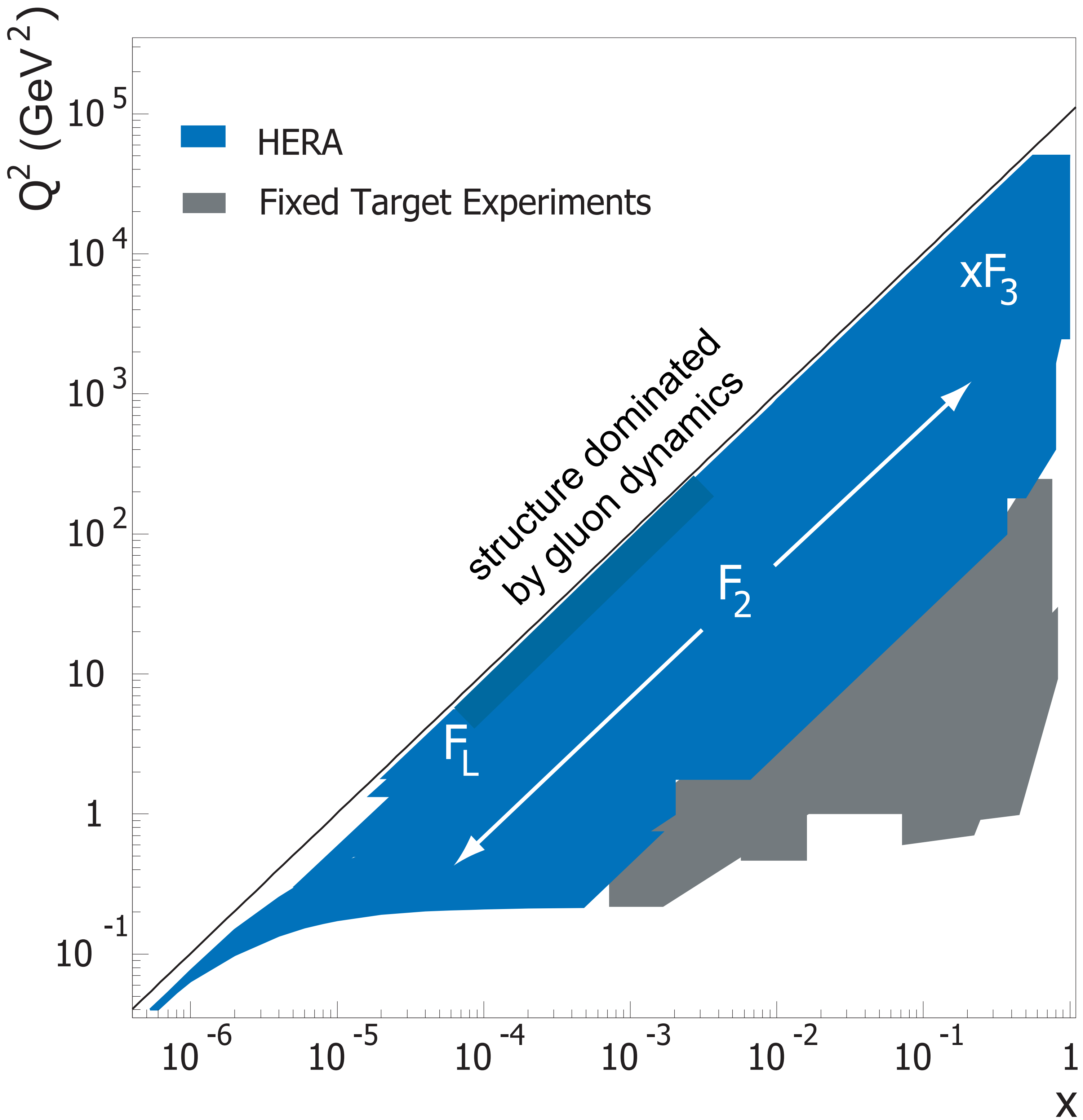

HERA data cover wide region of x,Q^2

<u>NC Measurements</u>
F_2 dominates most of Q^2 reach
xF_3 contributes in EW regime
F_L contributes only at highest y

<u>CC Measurements</u>
W_2 and xW_3 contribute equally
W_L only at high y

EW Couplings at LO

P_e = lepton beam polarisation

At LO in EW $\kappa = \dfrac{G_F m_Z^2}{2\sqrt{2}\pi\alpha}$

pure photon piece — interference piece — pure weak piece

$$\tilde{F}_2^{\pm} = F_2 - (v_e \pm P_e a_e)\kappa \frac{Q^2}{Q^2+M_Z^2} F_2^{\gamma Z} + (v_e^2 + a_e^2 \pm P_e 2 v_e a_e)\kappa^2 \left[\frac{Q^2}{Q^2+M_Z^2}\right]^2 F_2^Z$$

$$x\tilde{F}_3^{\pm} = -(a_e \pm P_e v_e)\kappa \frac{Q^2}{Q^2+M_Z^2} xF_3^{\gamma Z} + (2 a_e v_e \pm P_e [v_e^2 + a_e^2])\kappa^2 \left[\frac{Q^2}{Q^2+M_Z^2}\right]^2 xF_3^Z$$

interference piece — pure weak piece

v_e is small ~0.05
⇒ terms contribute little

$$\left[F_2, F_2^{\gamma Z}, F_2^Z\right] = x \sum_q [e_q^2, 2 e_q v_q, v_q^2 + a_q^2](q + \bar{q})$$

$$\left[xF_3^{\gamma Z}, xF_3^Z\right] = 2x \sum_q [e_q a_q, v_q a_q](q - \bar{q})$$

$F_2^{\gamma Z}$	→ main v_q constraint
F_2^Z	→ main constraint on a_q / v_q correlation
xF_3^Z	→ main a_q constraint

Structure Functions

NC data constrain:
- singlet quarks / gluon PDFs
- non-singlet valence quark PDFs at high Q^2

But, flavour sensitivity is weak

CC data enable flavour decomposition of proton:

$$W_2^- = x(u+c+\overline{d}+\overline{s})\,,\, W_2^+ = x(\overline{u}+\overline{c}+d+s)\,,$$
$$xW_3^- = x(u+c-\overline{d}-\overline{s})\,,\, xW_3^+ = x(d+s-\overline{u}-\overline{c})$$

Requires e^+ and e^- scattering data

$$\frac{d^2\sigma_{CC}^-}{dxdQ^2} = \frac{G_F^2}{2\pi}\left(\frac{M_W^2}{M_W^2+Q^2}\right)^2\left[(u+c)+(1-y)^2(\overline{d}+\overline{s})\right]$$

$$\frac{d^2\sigma_{CC}^+}{dxdQ^2} = \frac{G_F^2}{2\pi}\left(\frac{M_W^2}{M_W^2+Q^2}\right)^2\left[(\overline{u}+\overline{c})+(1-y)^2(d+s)\right]$$

For polarised lepton beams CC cross section scales linearly with P_e:

$\sigma_{CC}(e^-p) = 0$ for $P_e = +1$

$\sigma_{CC}(e^+p) = 0$ for $P_e = -1$

CC e+ data provide strong d_v constraint at high x (y ~ 0)

EW quark couplings

$e_q \; , a_q \; , v_q$

$$a_e = \sqrt{\rho_{NC}}\; I^3_{L,f}$$

$$v_e = \sqrt{\rho_{NC}}\; (I^3_{L,f} - 2 e_q \kappa_{NC,q} \sin^2\theta_W)$$

In on-shell scheme

$$\sin^2\theta_W = 1 - \frac{m_W^2}{m_Z^2}$$

$$G_F = \frac{\pi\alpha}{\sqrt{2} m_W^2} \frac{1}{\sin^2\theta_W} \frac{1}{(1-\Delta r)}$$

$$\Delta r = \Delta r(\alpha, m_W, m_Z, m_t, m_h, ...)$$

The $\rho_{NC,q}$ and $\kappa_{NC,q}$ are form factors — universal (fermion independent) functions of Q^2 and encapsulate HO EW loop effects,

$\rho_{CC,q} \; , \; \rho_{CC,\bar{q}}$ are inserted for quarks and anti-quarks in the above formulae account for HO EW effects (mainly loop effects)

$$W_2^- = x\left(\rho^2_{CC,eq} U + \rho^2_{CC,e\bar{q}} \overline{D}\right), \quad xW_3^- = x\left(\rho^2_{CC,eq} U - \rho^2_{CC,e\bar{q}} \overline{D}\right)$$

$$W_2^+ = x\left(\rho^2_{CC,eq} \overline{U} + \rho^2_{CC,e\bar{q}} D\right), \quad xW_3^+ = x\left(\rho^2_{CC,e\bar{q}} D - \rho^2_{CC,eq} \overline{U}\right)$$

$$U = u + c\,, \quad \overline{U} = \bar{u} + \bar{c}\,,$$

$$D = d + s\,, \quad \overline{D} = \bar{d} + \bar{s}$$

In SM extensions, form factors can be modified

$$\rho_{NC} \to \rho'_{NC}\rho_{NC}$$

$$\kappa_{NC} \to \kappa'_{NC}\kappa_{NC}$$

$$\rho_{CC} \to \rho'_{CC}\rho_{CC}$$

Can test for deviations beyond the SM

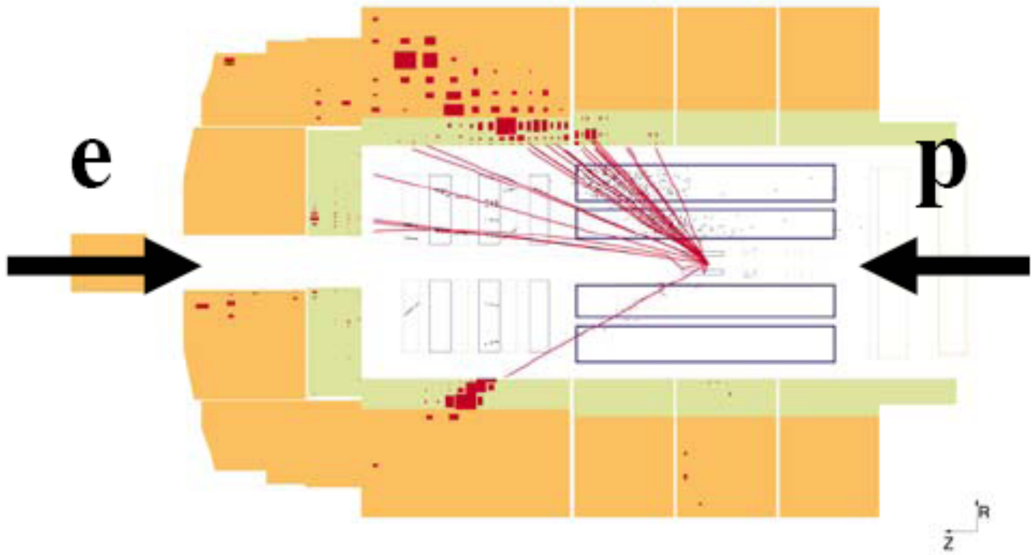

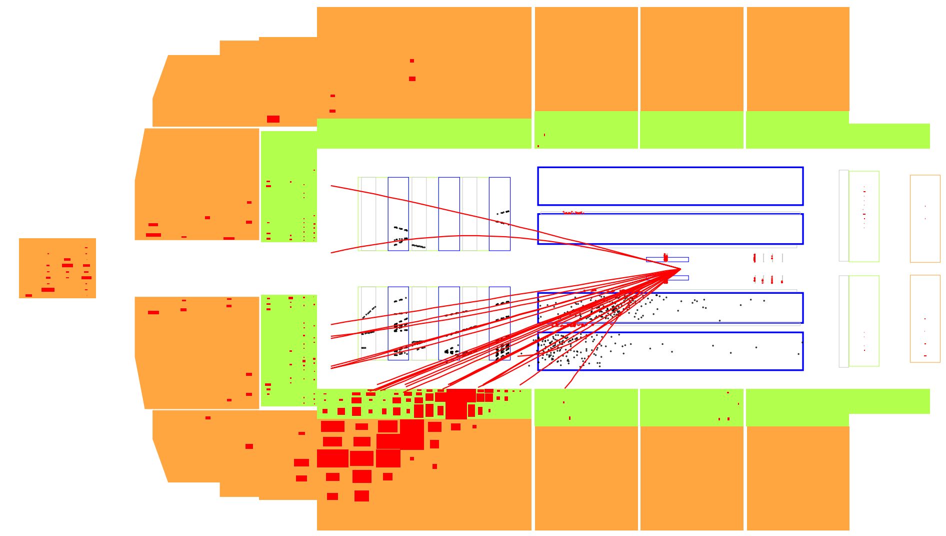

Neutral current event selection:

High P_T isolated scattered lepton
Suppress huge photo-production background by imposing longitudinal energy-momentum conservation

Kinematics may be reconstructed in many ways:
energy/angle of hadrons & scattered lepton
provides excellent tools for sys cross checks

Removal of scattered lepton provides a
high stats "pseudo-charged current sample"
Excellent tool to cross check CC analysis

Final selection: ~10^5 events per sample at high Q^2
~10^7 events for $10 < Q^2 < 100$ GeV^2

Charged current event selection:

Large missing transverse momentum (neutrino)

Suppress huge photo-production background

Topological finders to remove cosmic muons

Kinematics reconstructed from hadrons

Final selection: ~10^3 events per sample

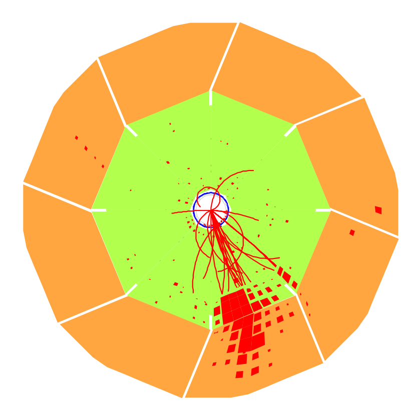

HERA Operation

<u>HERA-I operation 1993-2000</u>
Ee = 27.6 GeV
Ep = 820 / 920 GeV
$\int\mathcal{L}$ ~ 110 pb^{-1}

<u>HERA-II operation 2003-2007</u>
Ee = 27.6 GeV
Ep = 920 GeV
$\int\mathcal{L}$ ~ 330 pb^{-1}
Longitudinally polarised leptons

<u>Low Energy Run 2007</u>
Ee = 27.6 GeV
Ep = 575 & 460 GeV
Dedicated F_L measurement

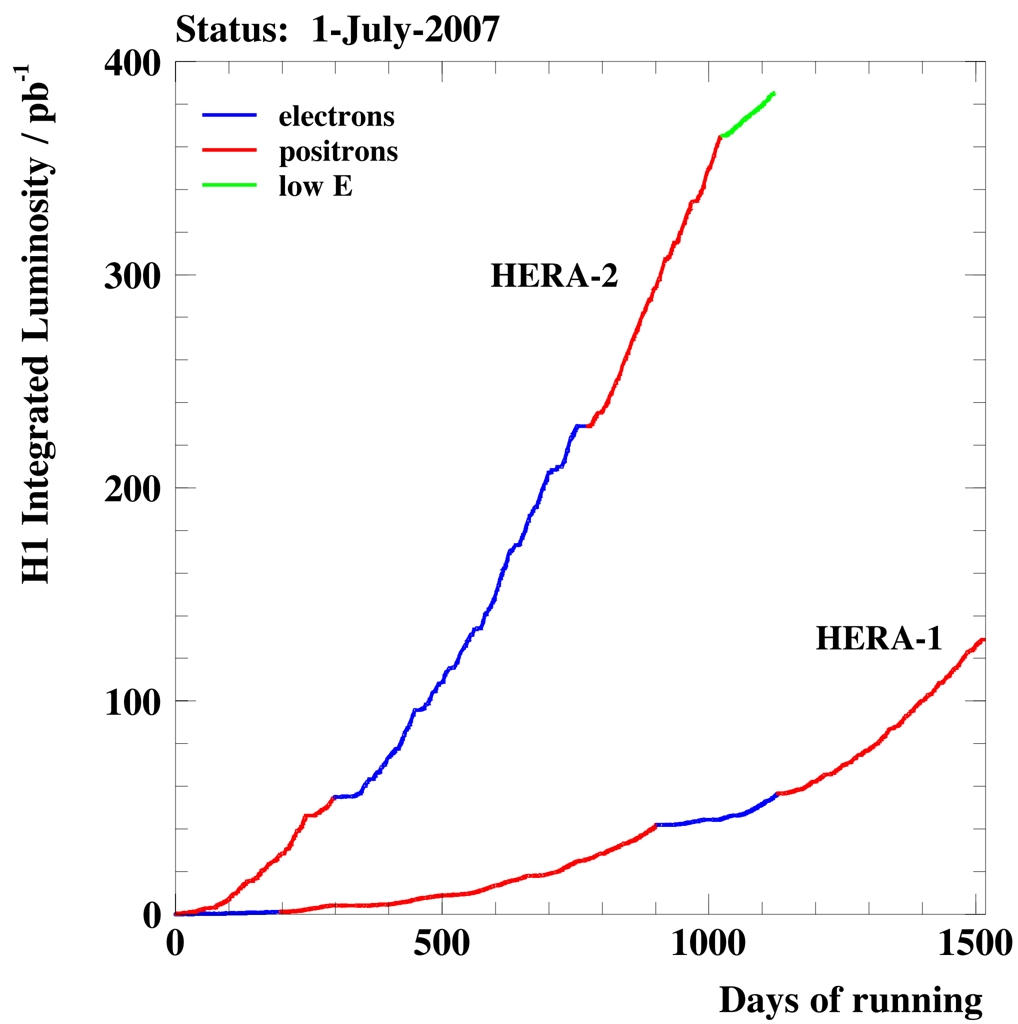

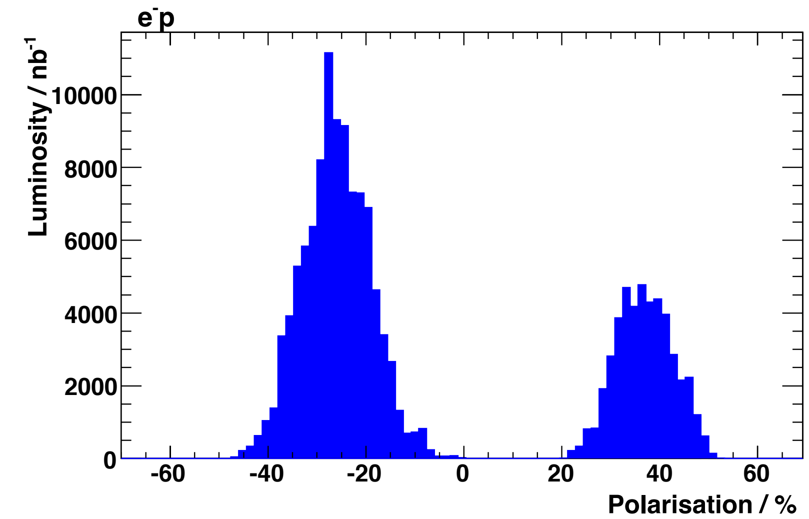

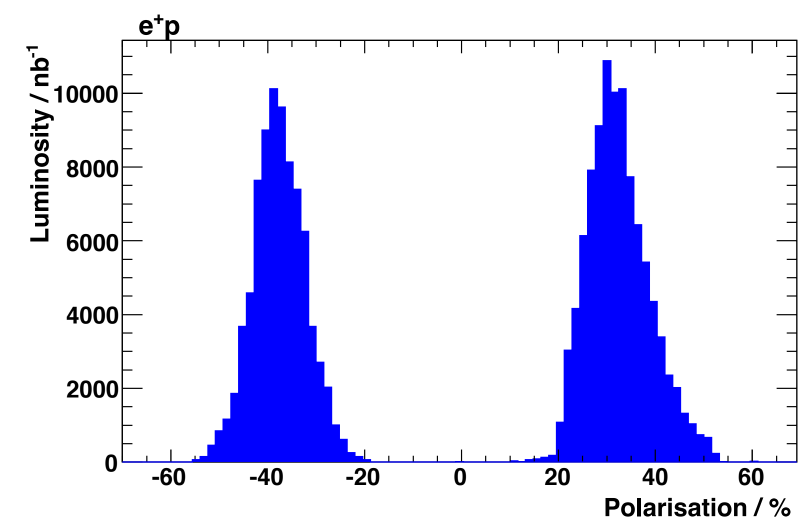

	R	L
e^-p	$\mathcal{L} = 45.9$ pb^{-1} $P_e = (+36.9 \pm 2.3)\%$	$\mathcal{L} = 103.2$ pb^{-1} $P_e = (-26.1 \pm 1.0)\%$
e^+p	$\mathcal{L} = 98.1$ pb^{-1} $P_e = (+32.5 \pm 1.2)\%$	$\mathcal{L} = 81.9$ pb^{-1} $P_e = (-37.6 \pm 1.4)\%$

First EW analysis performed on HERA-I data
This analysis includes:

- full HERA-1 and HERA-II dataset
- longitudinal lepton polarisation to enhance sensitivity
- factor 10 increase in e$^-$ & factor 3 increase in e$^+$ luminosity
- much improved systematic uncertainties

Datasets Used

	Data set	Q^2-range [GeV^2]	$\sqrt{s}$ [GeV]	$\mathcal{L}$ [pb^{-1}]	No. of data points	Polarisation [%]
1	e^+ combined low-Q^2	(0.5) 8.5 – 150	301,319	20, 22, 97.6	94 (262)	–
2	e^+ combined low-E_p	(1.5) 8.5 – 90	225,252	12.2, 5.9	132 (136)	–
3	e^+ NC 94–97	150 – 30 000	301	35.6	130	–
4	e^+ CC 94–97	300 – 15 000	301	35.6	25	–
5	e^- NC 98–99	150 – 30 000	319	16.4	126	–
6	e^- CC 98–99	300 – 15 000	319	16.4	28	–
7	e^- NC 98–99 high-y	100 – 800	319	16.4	13	–
8	e^+ NC 99–00	150 – 30 000	319	65.2	147	–
9	e^+ CC 99–00	300 – 15 000	319	65.2	28	–
10	e^+ NC L HERA-II	120 – 30 000	319	80.7	136	−37.0 ± 1.0
11	e^+ CC L HERA-II	300 – 15 000	319	80.7	28	−37.0 ± 1.0
12	e^+ NC R HERA-II	120 – 30 000	319	101.3	138	+32.5 ± 0.7
13	e^+ CC R HERA-II	300 – 15 000	319	101.3	29	+32.5 ± 0.7
14	e^- NC L HERA-II	120 – 50 000	319	104.4	139	−25.8 ± 0.7
15	e^- CC L HERA-II	300 – 30 000	319	104.4	29	−25.8 ± 0.7
16	e^- NC R HERA-II	120 – 30 000	319	47.3	138	+36.0 ± 0.7
17	e^- CC R HERA-II	300 – 15 000	319	47.3	28	+36.0 ± 0.7
18	e^+ NC HERA-II high-y	60 – 800	319	182.0	11	–
19	e^- NC HERA-II high-y	60 – 800	319	151.7	11	–

Low Q^2 data constrain PDFs

HERA-I

HERA-II

Unpolarised High Q^2 NC Cross Sections

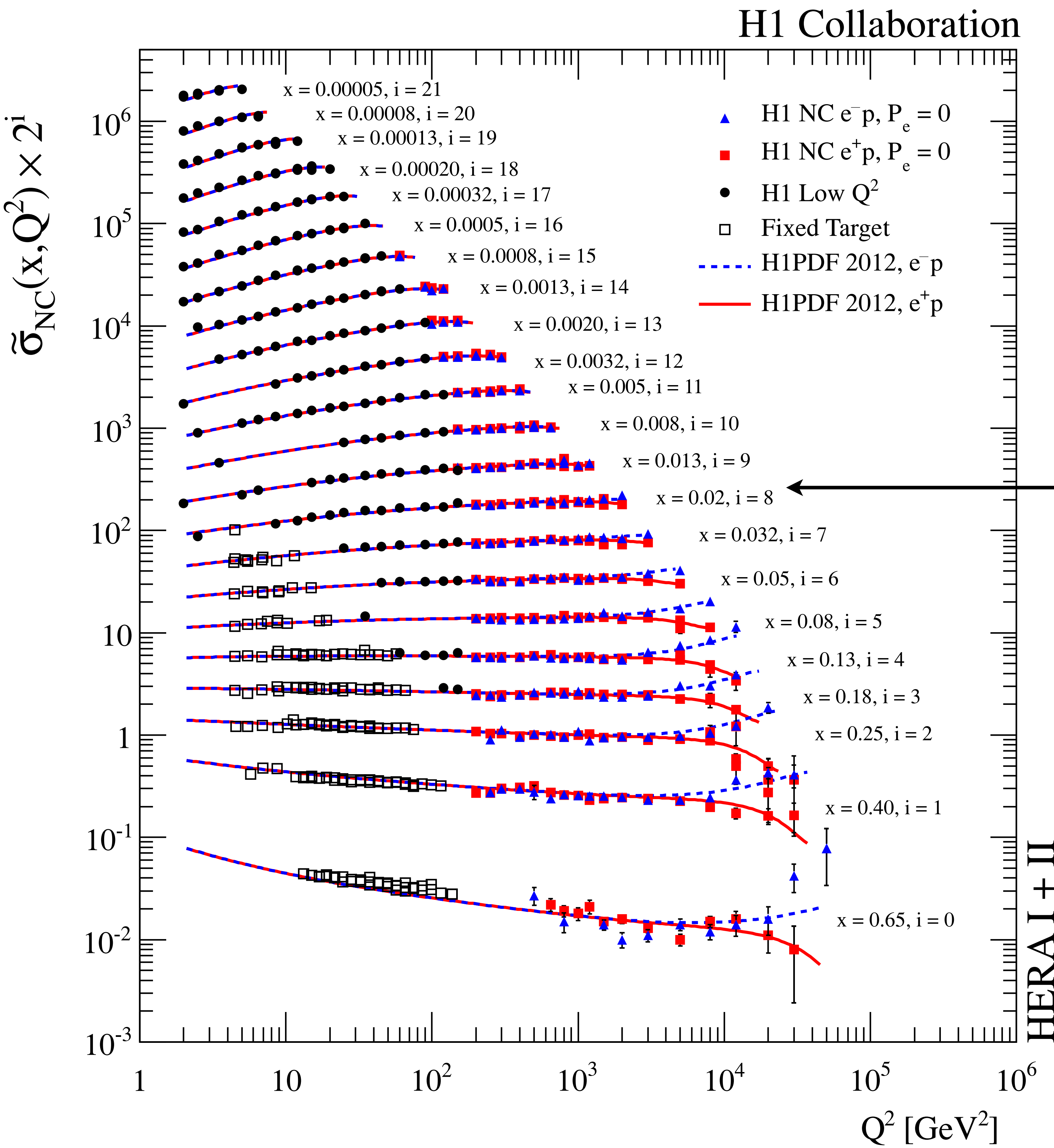

H1 precision 1.5% for $Q^2 < 500$ GeV^2
⇒ factor 2 reduction in error wrt HERA-I

Statistics limited at higher Q^2 and high x

Extended reach at high x

This x region is the 'sweet spot'
High precision with long Q^2 lever arm
x-range relevant for Higgs production

Combination of high Q^2 data
HERA-I and HERA-II

Larger HERA-II luminosity
→ improved precision at high x / Q^2

Data well described by NLO QCD in this case H1PDF2012 — qualitatively similar to HERAPDF

Electron scattering

$$\frac{d^2\sigma^-_{CC}}{dxdQ^2} = \frac{G_F^2}{2\pi}\left(\frac{M_W^2}{M_W^2+Q^2}\right)^2\left[(u+c)+(1-y)^2(\bar{d}+\bar{s})\right]$$

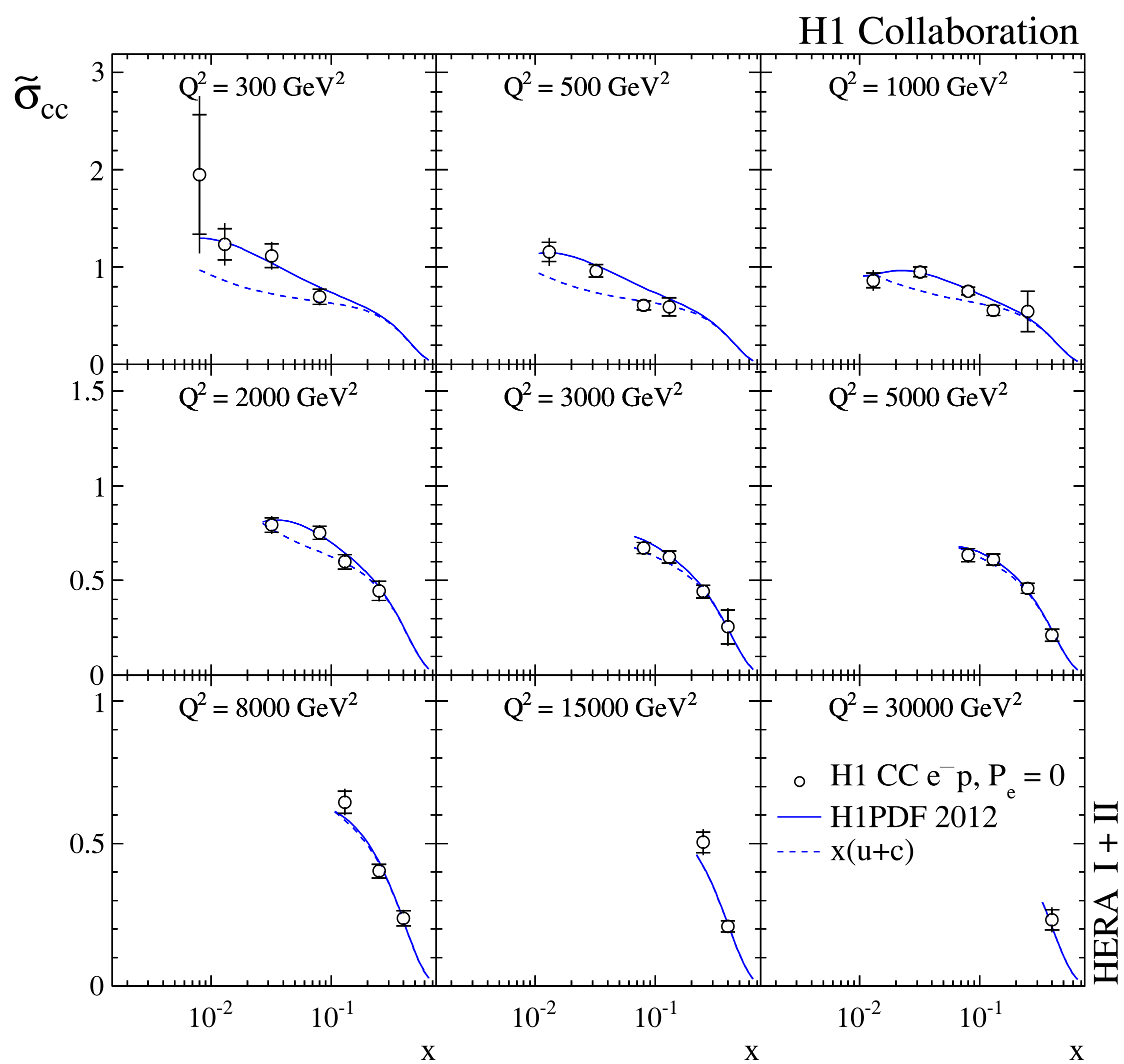

Positron scattering

$$\frac{d^2\sigma^+_{CC}}{dxdQ^2} = \frac{G_F^2}{2\pi}\left(\frac{M_W^2}{M_W^2+Q^2}\right)^2\left[(\bar{u}+\bar{c})+(1-y)^2(d+s)\right]$$

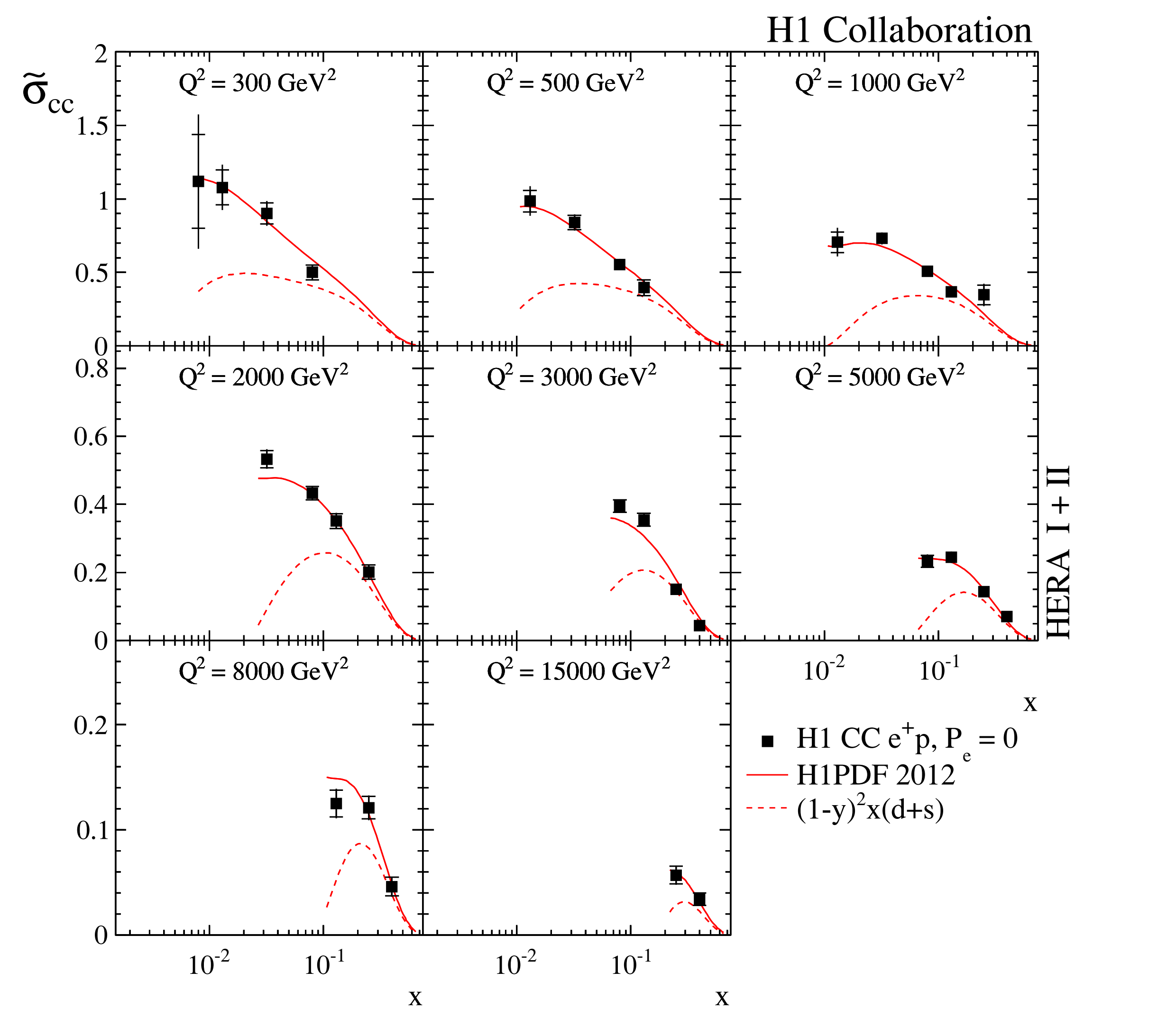

H1 combination of high Q^2 CC data (HERA-I+II)
Improvement of total uncertainty
Dominated by statistical errors
Provide important flavour decomposition information

CC e+ data provide strong d_v constraint at high x
Precision limited by statistics: typically 5-10%
HERA-I precision of 10-15% for e+p

Fit Methodology - NNLO QCD ⊗ NLO EW Fit

Dedicated PDF fit required to avoid bias (EW params used in PDF fits)
Combine NC and CC HERA-I data from H1
Complete MSbar NNLO QCD fit
$\alpha_s = 0.1176$ (fixed in fit)

- Combined QCD / EW fit accounts for correlations in uncertainties
- Fits constructed very similar to HERAPDF2.0 at NNLO QCD

Each PDF parameterised by form

$$xf(x,Q_0^2) = A \cdot x^B \cdot (1-x)^C \cdot (1 + Dx + Ex^2)$$

xg, xu_v, xd_v, $x\bar{U}$, $x\bar{D}$ →

$$\begin{aligned} xg(x) &= A_g x^{B_g}(1-x)^{C_g} - A'_g x^{B'_g}(1-x)^{C'_g} \\ xu_v(x) &= A_{u_v} x^{B_{u_v}}(1-x)^{C_{u_v}}(1+E_{u_v}x^2), \\ xd_v(x) &= A_{d_v} x^{B_{d_v}}(1-x)^{C_{d_v}}, \\ x\bar{U}(x) &= A_{\bar{U}} x^{B_{\bar{U}}}(1-x)^{C_{\bar{U}}}, \\ x\bar{D}(x) &= A_{\bar{D}} x^{B_{\bar{D}}}(1-x)^{C_{\bar{D}}} \end{aligned}$$

13 free PDF params. + 4 polarisation params.
1410 measurements + 4 polarisation measurements

$$\chi^2/n_{\rm dof} = 1432/(1414-17) = 1.03$$

Excellent consistency of data allows standard statistical error definition: $\Delta\chi^2 = 1$

Apply momentum/counting sum rules:

$$\int_0^1 dx \cdot (xu_v + xd_v + x\bar{U} + x\bar{D} + xg) = 1$$

$$\int_0^1 dx \cdot u_v = 2 \qquad \int_0^1 dx \cdot d_v = 1$$

Parameter constraints:
$A_{Ubar} = A_{Dbar}$
$B_{Ubar} = B_{Dbar}$
sea = 2 x (Ubar +Dbar)
$C'_g = 25$ (fixed)

$Q_0^2 = 1.9$ GeV^2 (below m_c)
$Q^2 > 8.5$ GeV^2
$2 \times 10^{-4} < x < 0.65$
Fits performed using ZM-VFNS

Perform fit to W mass - sensitivity mainly from CC cross section normalisation (i.e. via G_F)

$$m_W = 80.520 \pm 0.070_{\rm stat} \pm 0.055_{\rm syst} \pm 0.074_{\rm PDF} [\pm 0.115_{\rm total}] {\rm GeV}$$

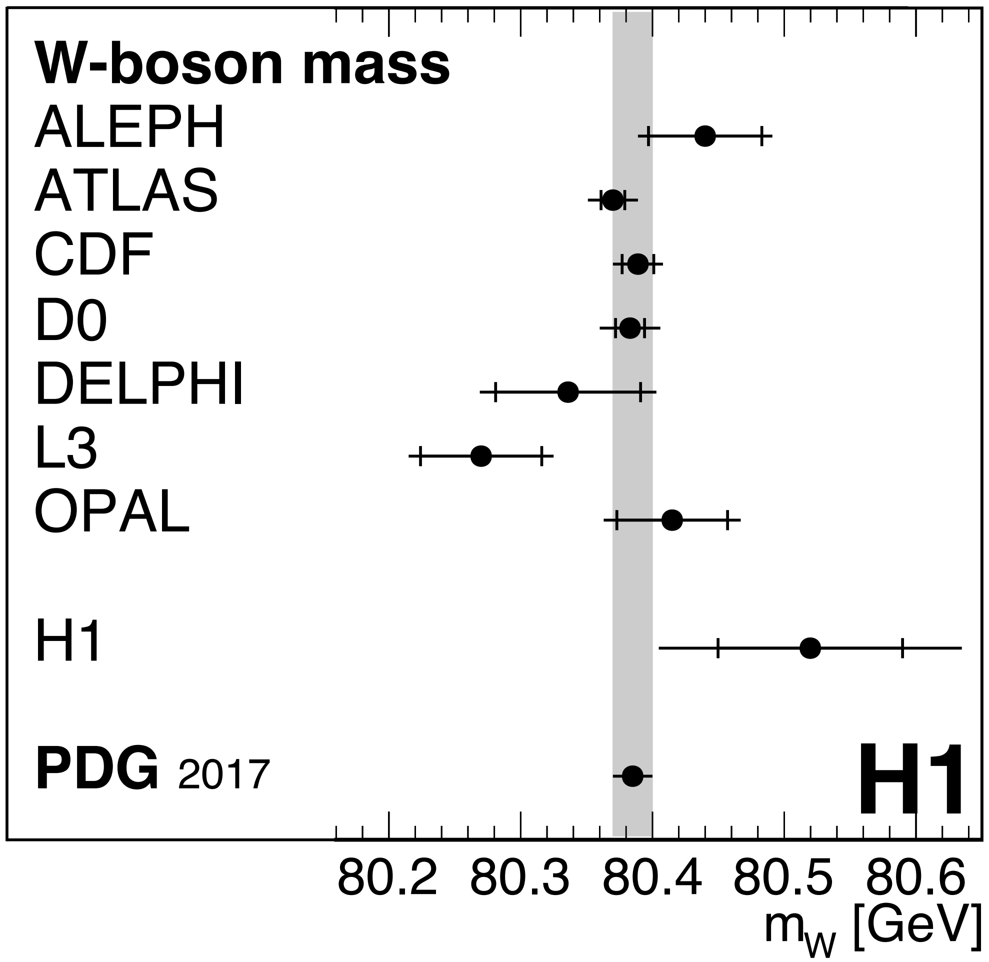

Indirect measurement of m_W, or equivalently $\sin^2\theta_W$:

$\sin^2\theta_W = 0.022029 \pm 0.002233$

in on-shell scheme

$$G_F = \frac{\pi\alpha}{\sqrt{2} m_W^2} \frac{1}{\sin^2\theta_W} \frac{1}{(1-\Delta r)}$$

$$\Delta r = \Delta r(\alpha, m_W, m_Z, m_t, m_h, ...)$$

$$\frac{d^2\sigma_{CC}}{dxdQ^2} \propto \frac{G_F^2}{2\pi} \left(\frac{M_W^2}{M_W^2 + Q^2} \right)^2$$

Can also test the space-like charged current propagator mass = 80.62 ± 0.79 GeV

Weak Couplings

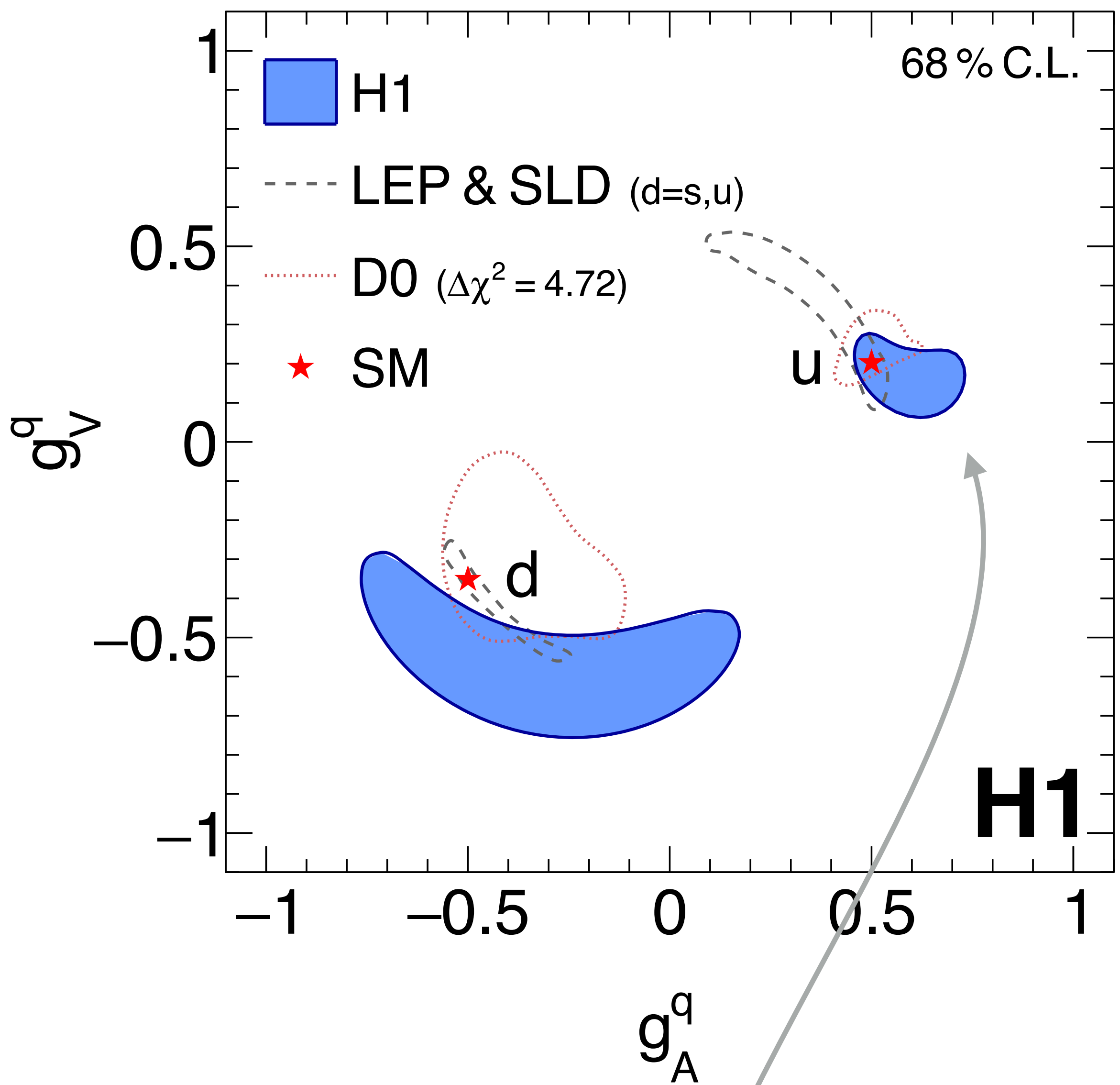

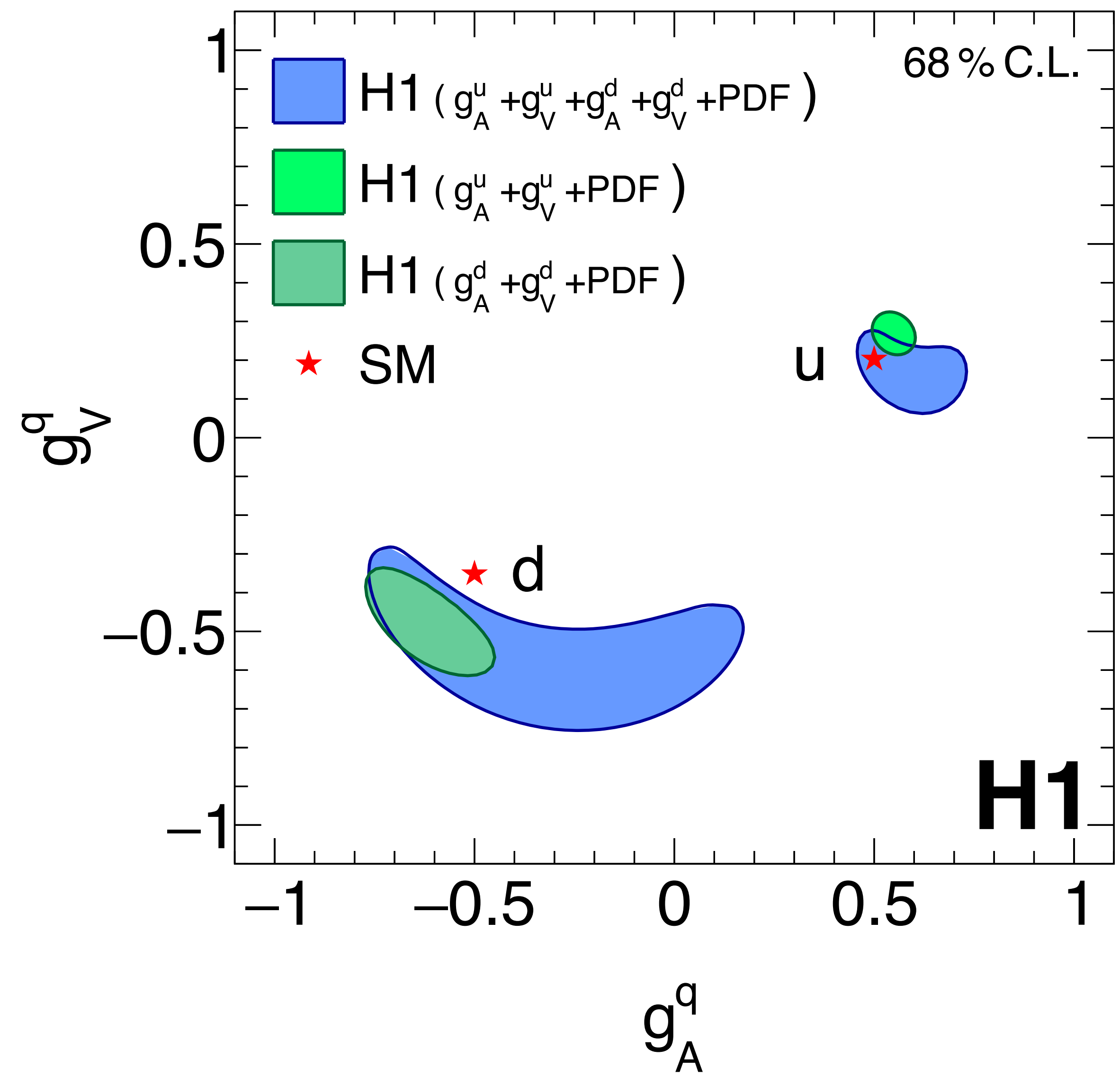

Perform 4-coupling and two 2-coupling fits:

4-coupling fits extract u,d axial and vector couplings

α, m_W, m_Z, m_t, m_H are taken as other input EW parameters

2-coupling fit extracts u-type axial / vector couplings

2-coupling fit extracts d-type axial / vector couplings

Similar sensitivity to g_V^u and g_A^u as LEP and D0

$$g_A^q = \sqrt{\rho_{\mathrm{NC},q}} I^3_{\mathrm{L},q} ,$$
$$g_V^q = \sqrt{\rho_{\mathrm{NC},q}} \left(I^3_{\mathrm{L},q} - 2 Q_q \kappa_{\mathrm{NC},q} \sin^2\theta_W \right)$$

$$\rho_{\mathrm{NC}} \to \rho'_{\mathrm{NC}} \rho_{\mathrm{NC}}$$
$$\kappa_{\mathrm{NC}} \to \kappa'_{\mathrm{NC}} \kappa_{\mathrm{NC}}$$
$$\rho_{\mathrm{CC}} \to \rho'_{\mathrm{CC}} \rho_{\mathrm{CC}}$$

Neutral current

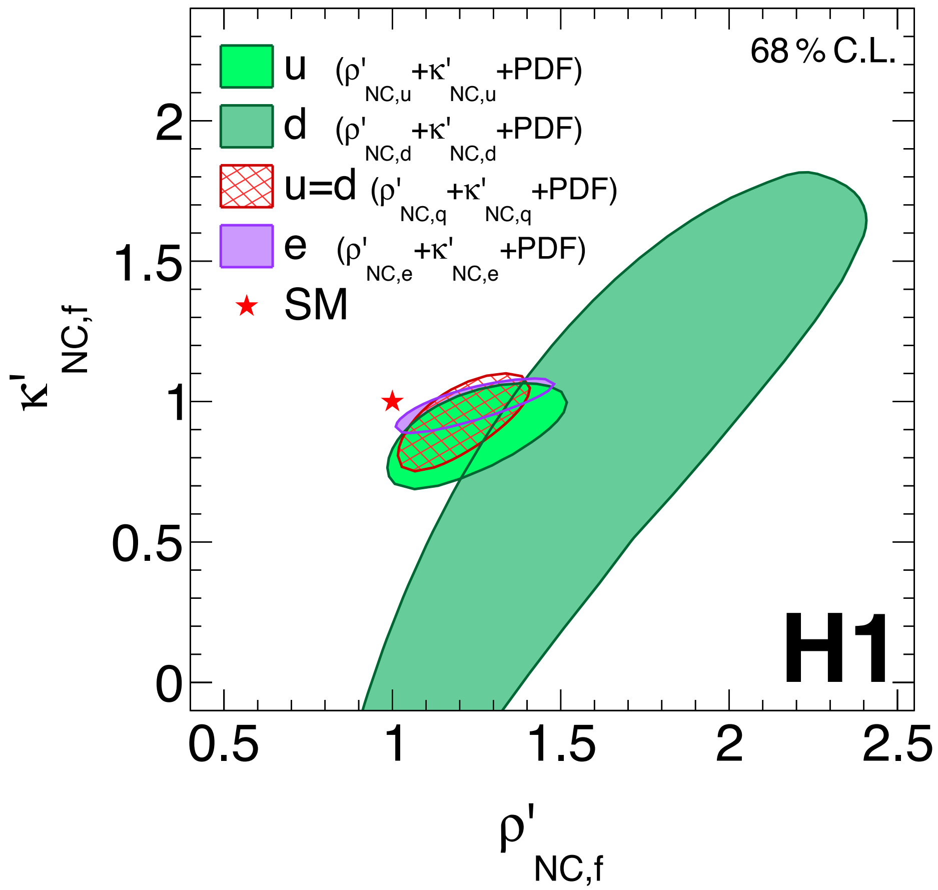

Charged current

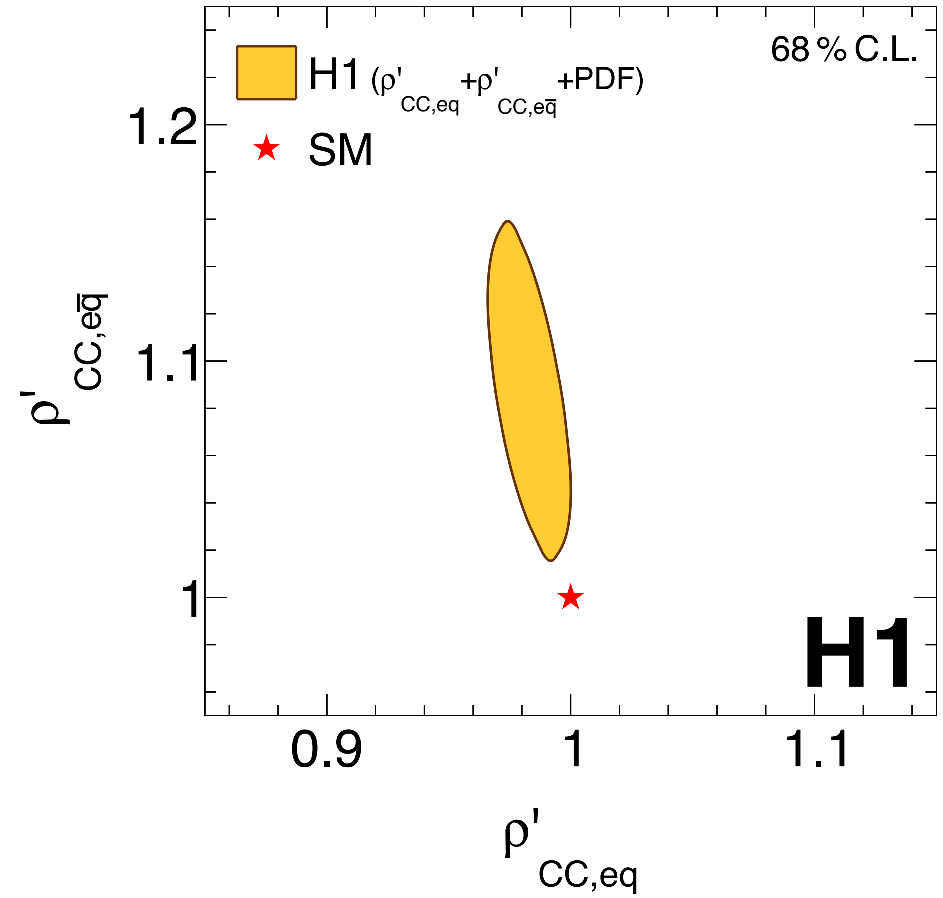

Perform 4 variants of NC fits
- u-type form factors fitted
- d-type form factors fitted
- u-type = d-type form factors
- electron form factors fitted

All fits consistent with SM < 2 std deviations
d-type fits have larger uncertainty
- → lower d charge ±⅓
- → smaller contribution to cross section
- → smaller d density in proton

α, m_W, m_Z, m_t, m_H fixed to SM values
Unfitted ρ' and κ' set to unity

Perform 1 CC fit
high sensitivity to ρ'_{eq} of ~2%
lower sensitivity to ρ'_{eqbar} due to smaller cross section

Consistency with SM at level of ~1σ

Scale Dependence of NC Weak Form Factors

Divide data with Q^2>500 GeV^2 into four Q^2 bins to probe scale dependence

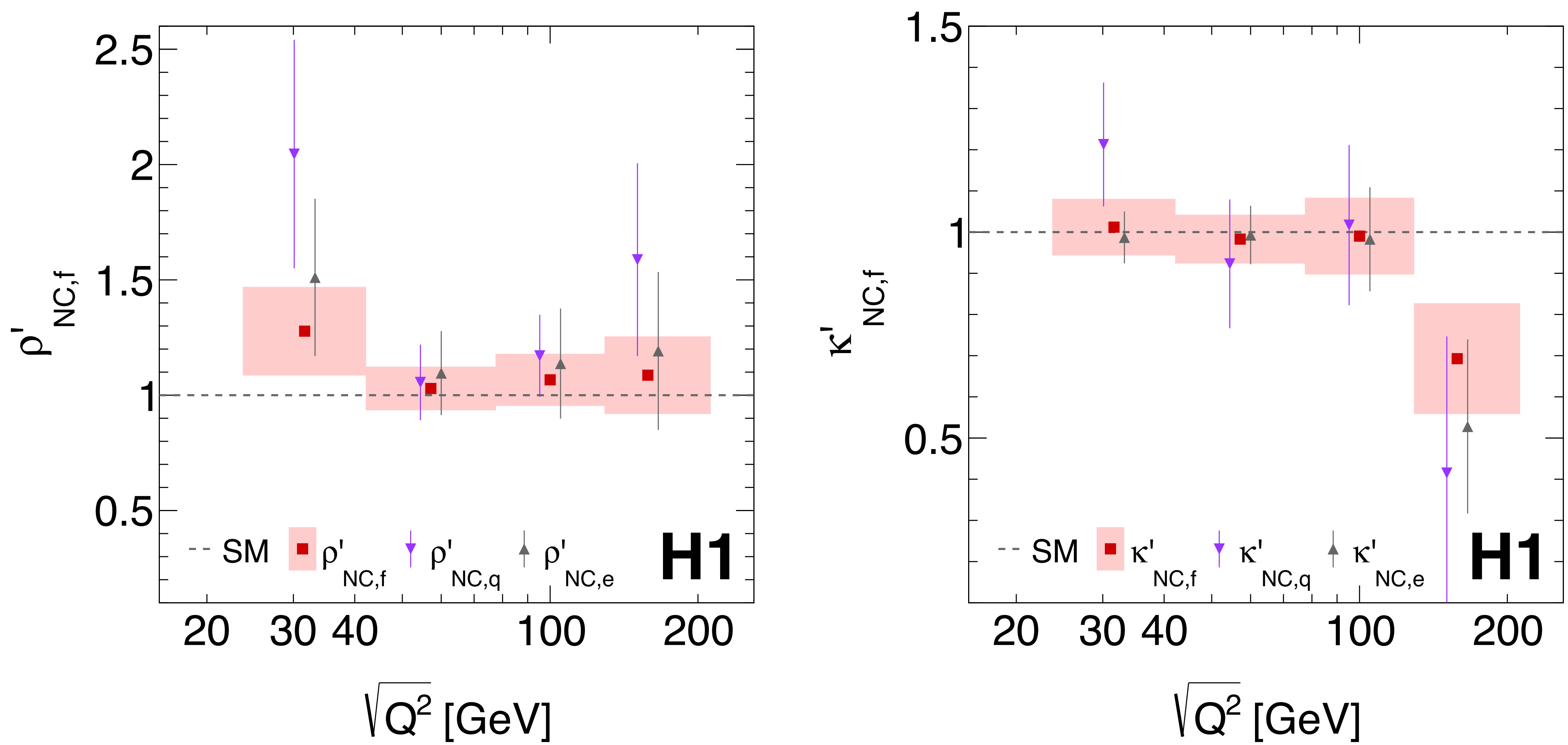

Can repeat fits in bins of Q^2 scale of DIS data:

1. fit PDFs and quark form factors
2. fit PDFs and electron form factors
3. fit PDFs and common fermion form factors

Error bars / bands show full uncertainties

Set ρ' and κ' = unity for Q^2<500 GeV^2

Best sensitivity at Q~60 GeV of ~6%

Results consistent with SM at <1.5σ

Scale Dependence of CC Weak Form Factors

First test of flavour and scale dependence of CC weak form factors

All CC data divided into four Q^2 bins to probe scale dependence

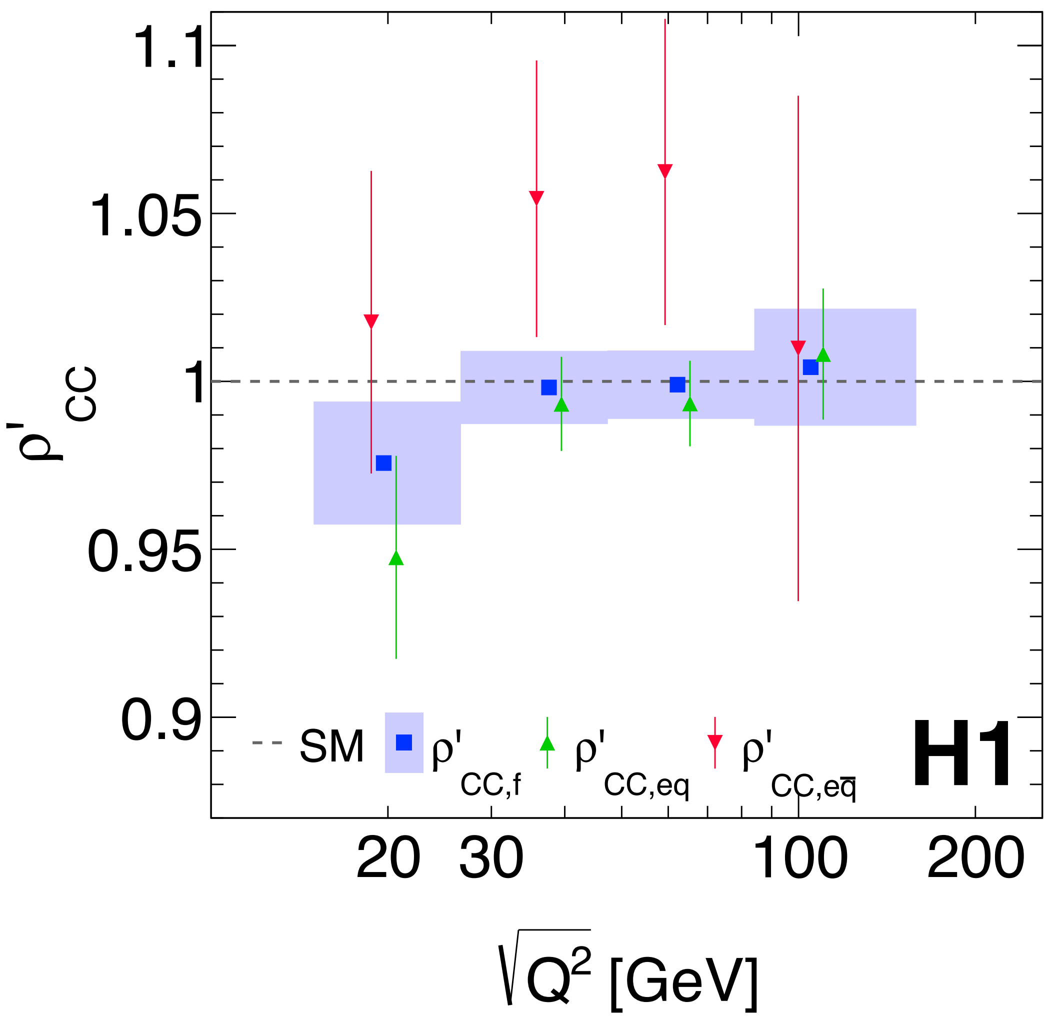

Repeat fits in bins of Q^2 scale of DIS data:

1. fit PDFs and eq form factors
2. fit PDFs and eqbar form factors
3. fit PDFs and common fermion form factors

Error bars / bands show full uncertainties

Precision on ρ'_{eqbar} ~ 4%
Precision on ρ'_{eq} ~ 1.3 — 3%
Precision on ρ'_{f} ~ 0.8 — 1.8%

No significant deviations from SM

Summary

This study completes analysis of legacy HERA polarised data

Light quark weak couplings consistent with SM
Analysis tests complementarity of time-like and space-like regimes
H1 sensitivity similar to Tevatron and LEP

Search of indirect BSM effects in weak coupling scale dependencies
First determination of scale and flavour dependence in CC DIS
No significant deviations from SM observed

arXiv:1806.01176
Submitted to EPJC

Backup

Higher Order EW Corrections

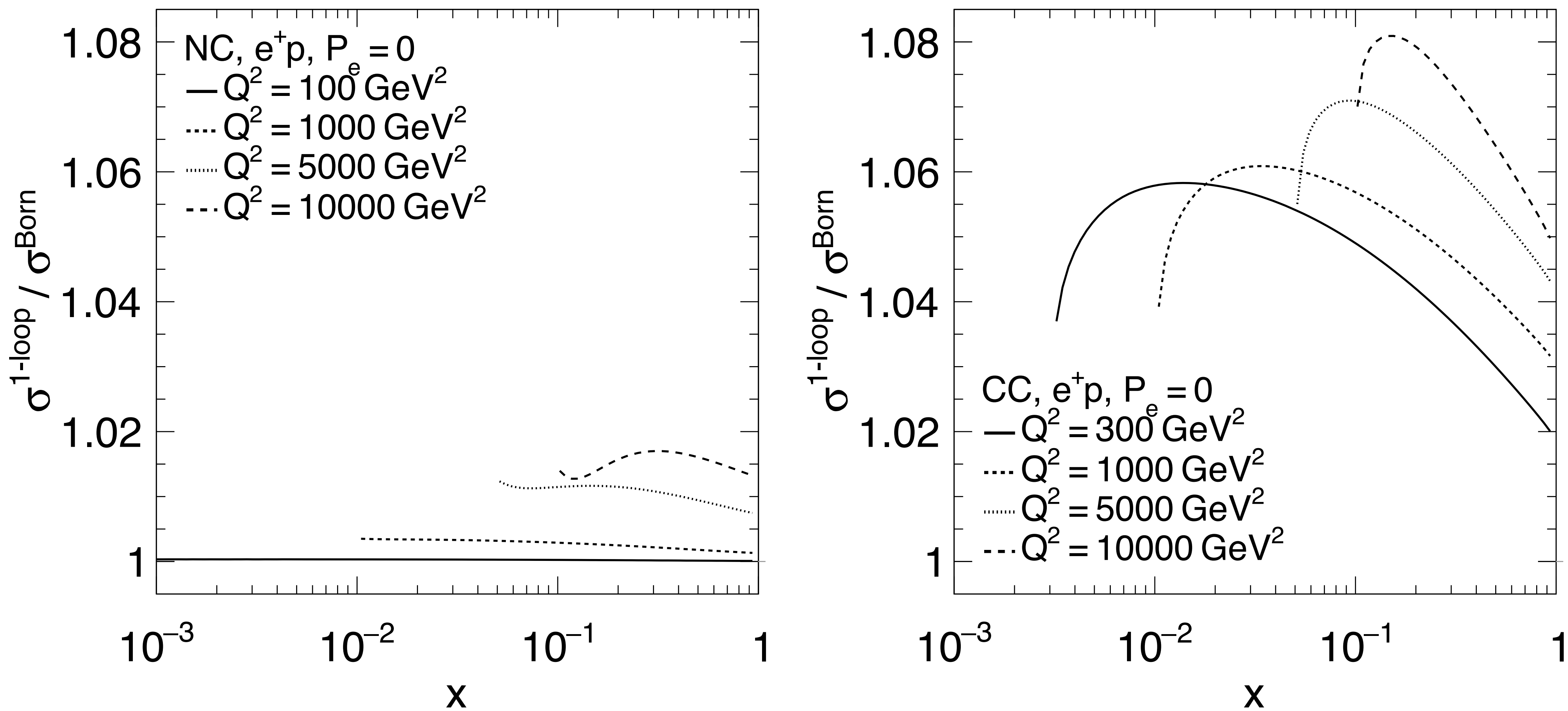

Size of 1-loop EW corrections for NC and CC vs Q^2 (excl. vacuum polarisation & virtual photon corrections)
Corrections vary by < 0.1% for polarised case, or for e^- scattering

Electroweak Precision Observables - $\sin^2\theta_{eff}$

$\sin^2\theta_W$ is a fundamental parameter of the SM - specifies the mixing between EM and weak fields
Relates the Z and W couplings g_Z and g_W (and their masses)

At leading order $$\sin^2\theta_W = 1 - \frac{g_W^2}{g_Z^2} = 1 - \frac{m_W^2}{m_Z^2}$$

Higher order EW corrections modify this to an effective mixing angle dependent on fermion flavour ***f***

$$\sin^2\theta^f_{\rm eff} = (1 - \frac{m_W^2}{m_Z^2}) \cdot (1 + \Delta r)$$

Δr encapsulates radiative corrections
Is EW scheme dependent

With known m_h EW sector of SM is over-constrained

- m_Z = 91.1876 GeV
- G_μ = 1.16637 x 10^{-5} GeV^{-2}
- $\alpha_{QED}(0)$ = 1/137.035

$$m_{\rm W}^2 = \frac{\pi\alpha(0)}{\sqrt{2}G_\mu \sin^2\theta_{\rm W}} \frac{1}{1-\Delta r}$$

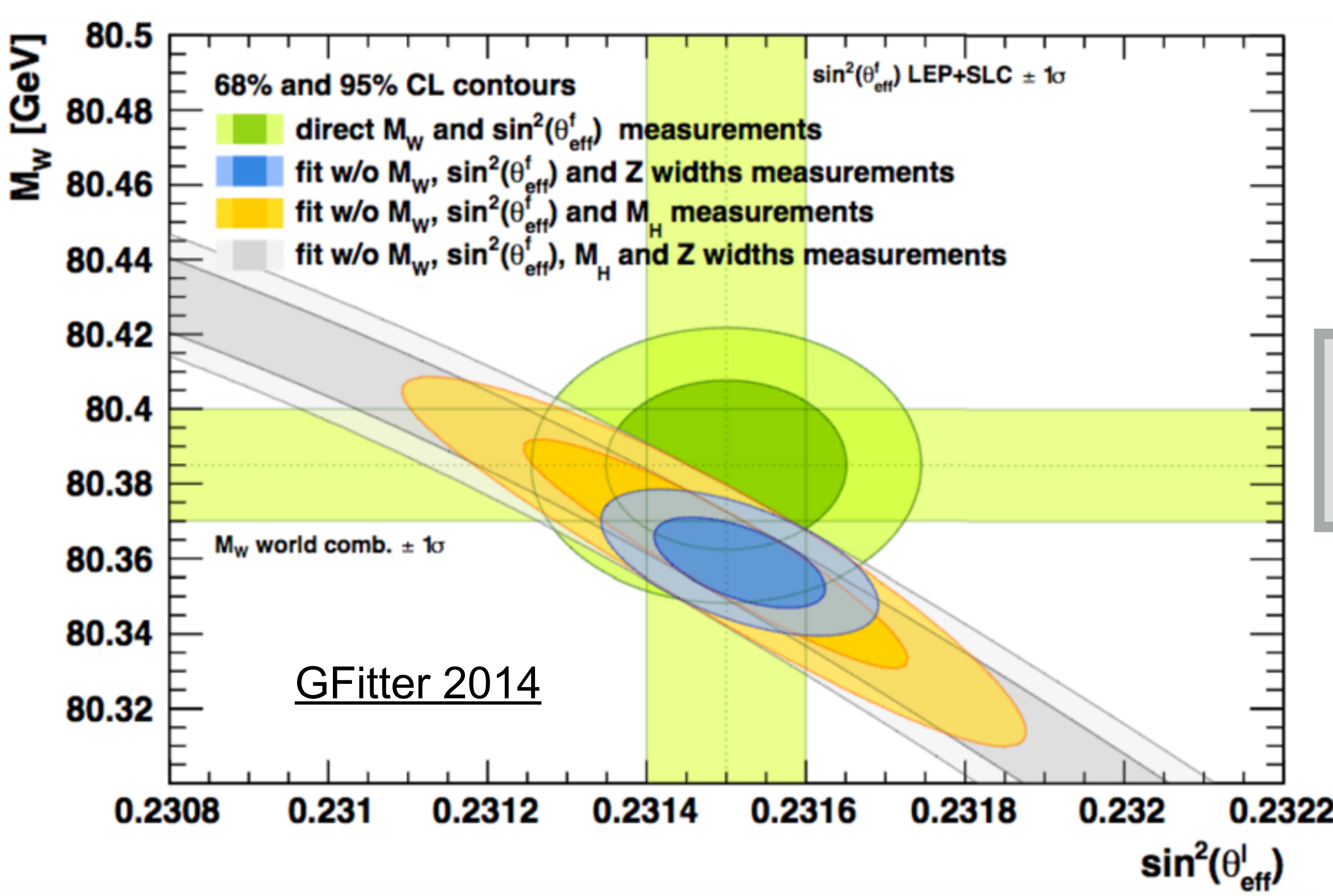

EW scheme dependent corrections incorporated into $\Delta r \rightarrow \Delta r(m_H, m_{top}$, new physics)
Measurement of one observable can predict the other
$m_W \Leftrightarrow \sin^2\theta_W$

> m_W and $\sin^2\theta_{eff}$ allows self-consistency check of SM
> New physics may hide in the indirect higher order corrections
> Valuable in absence of direct signals

Previous results on $\sin^2\theta_{eff}$

LEP:	29 x10^{-5}	CDF/D0:	35 x10^{-5}
SLD:	26 x10^{-5}	CMS(7TeV):	320 x10^{-5}
		ATLAS(7TeV):	120 x10^{-5}

> Uncertainty of ± 50x10^{-5} in $\sin^2\theta_{eff}$ is equivalent to ± 25 MeV in m_W

Extracting $\sin^2\theta_{eff}$

Typically experiments measure A_{FB}
→ unfold detector effects / dilution → fit for $\sin^2\theta_{eff}$
→ or, perform detector level template fits to A_{FB}
→ estimate PDF uncertainties on extraction

D0 + CDF combination 2017

$$\sin^2\theta_{\rm eff}^{\rm lept} = 0.23148 \pm 0.00027\ ({\rm stat.}) \pm 0.00005\ ({\rm syst.}) \pm 0.00018\ ({\rm PDF})$$

At LHC / Tevatron largest uncertainty ~ PDFs
worse at LHC due to pp collisions
worse at larger √s due to lower x (more dilution)

ATLAS 7 TeV

$$\sin^2\theta_{\rm eff}^{\rm lept} = 0.2308 \pm 0.0005({\rm stat.}) \pm 0.0006({\rm syst.}) \pm 0.0009({\rm PDF}) = 0.2308 \pm 0.0012({\rm tot.})$$

CMS 7 TeV

$$\sin^2\theta_{\rm eff} = 0.2287 \pm 0.0020\ ({\rm stat.}) \pm 0.0025\ ({\rm syst.})$$

dominated by PDF (±0.00130)

LHCb 7 & 8 TeV

$$\sin^2\theta_{\rm W}^{\rm eff} = 0.23142 \pm 0.00073({\rm stat}) \pm 0.00052({\rm sys}) \pm 0.00056({\rm theo})$$

dominated by PDF

GFitter 2014

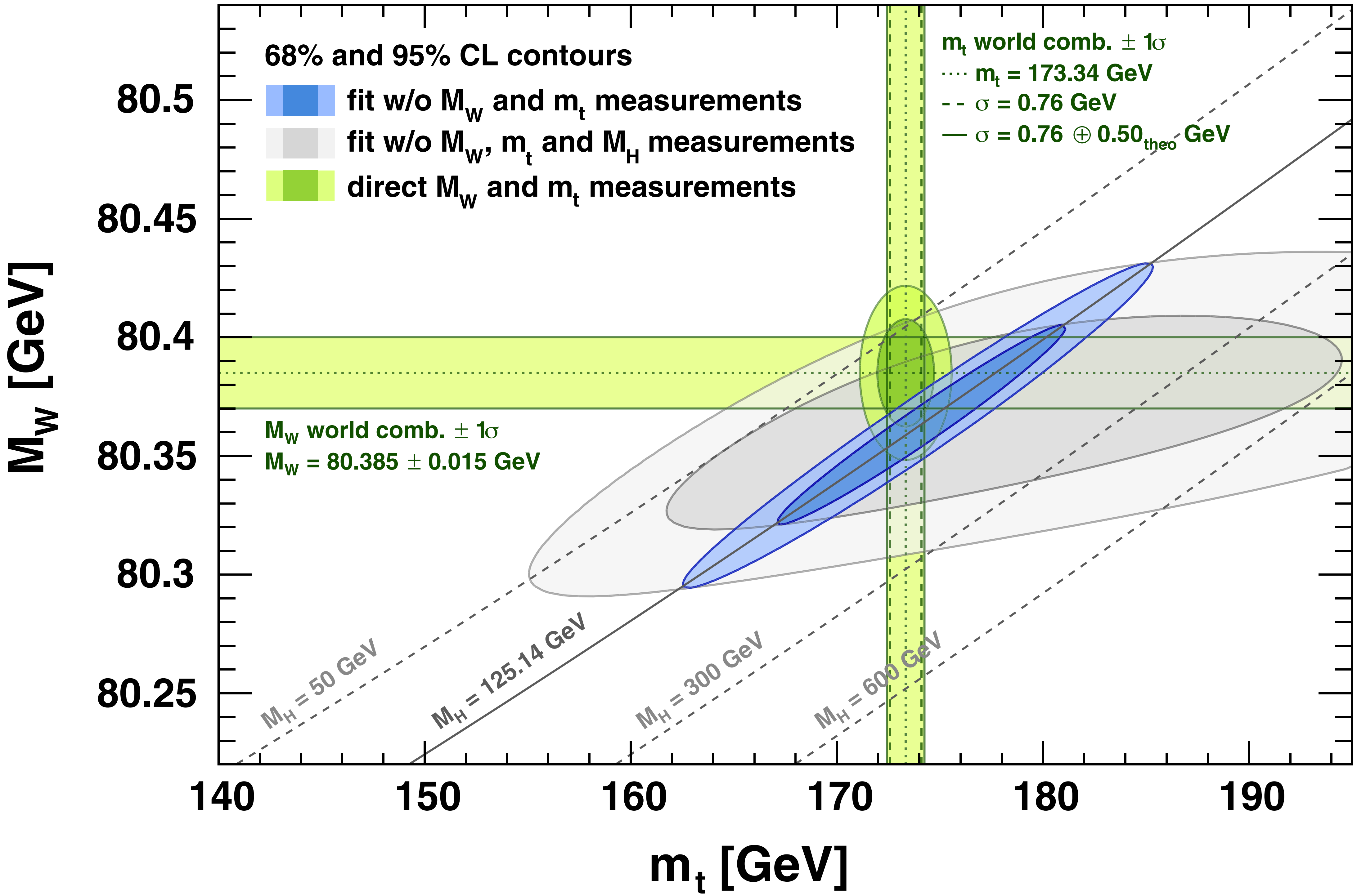

Direct measurements compared to EW fits and indirect constraints

Electroweak Precision Observables - m_W

New ATLAS measurement of m_W reaches ±19 MeV precision arXiv:1701.07240

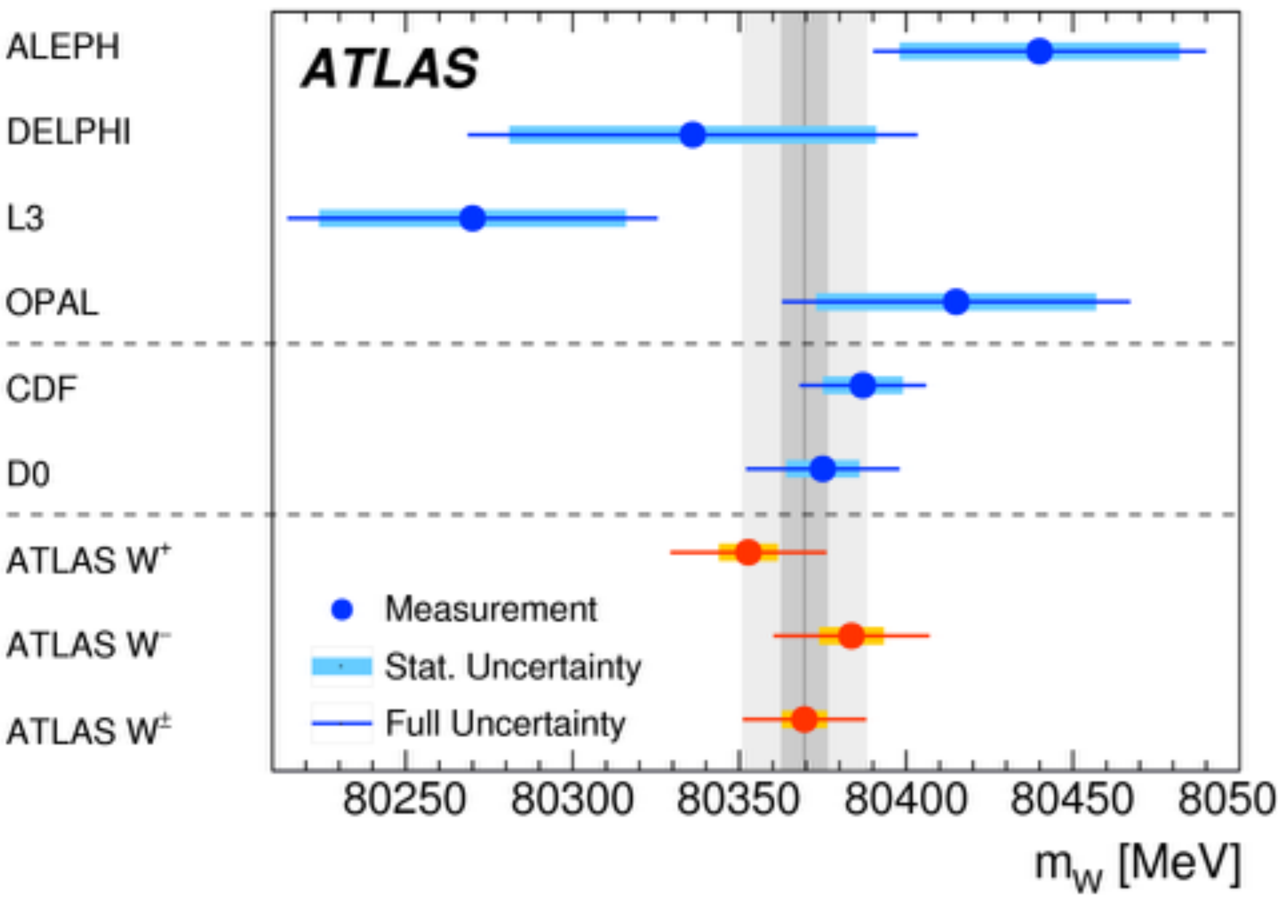

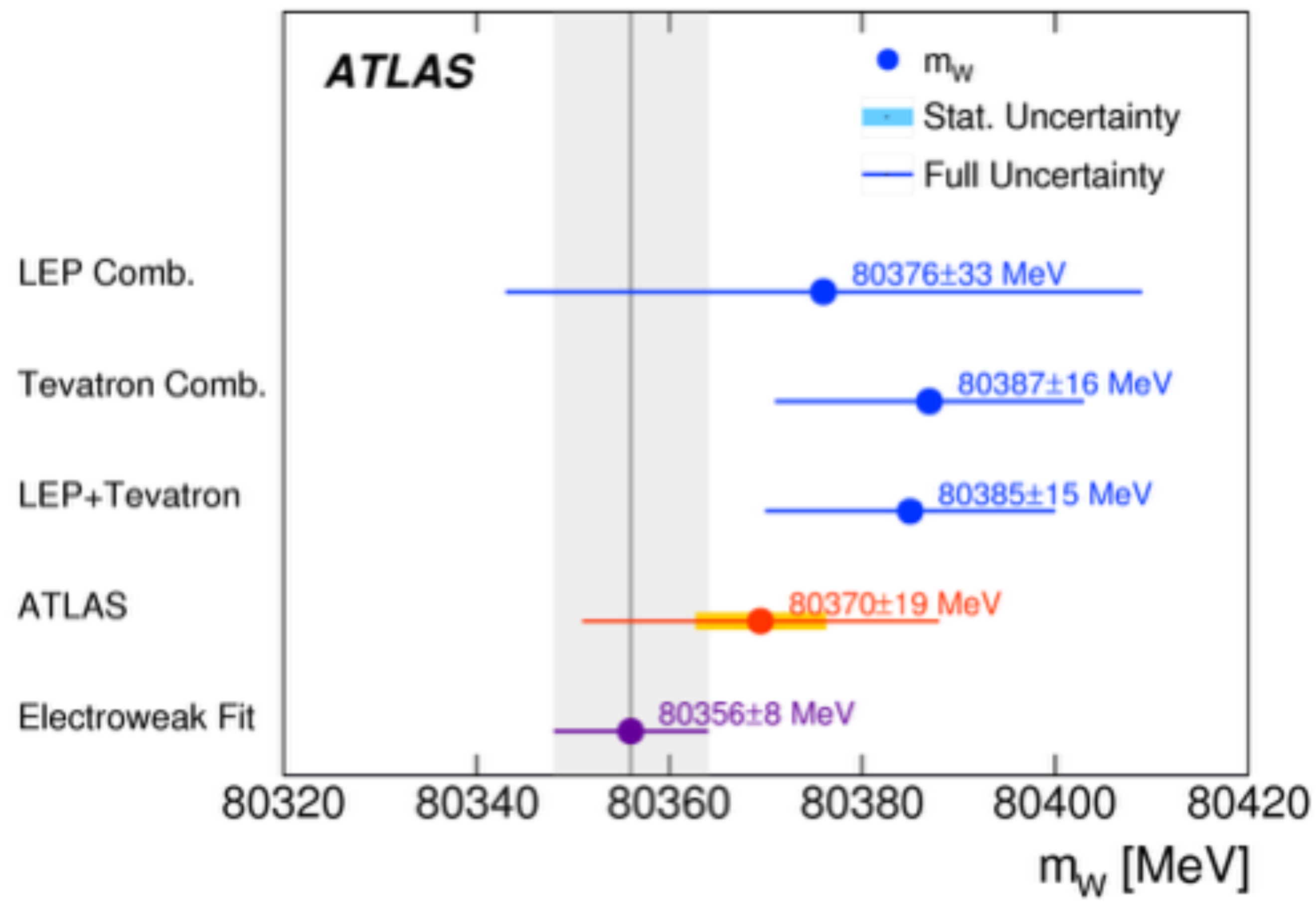

ATLAS approaches precision of combined LEP + Tevatron measurement
Theory prediction from EW fit has uncertainty ±8 MeV